RESEARCH ARTICLE

Nuclear accumulation of mRNAs underlies G4C2-repeat-induced translational repression in a cellular model of *C9orf72* ALS

Simona Rossi[1,2,3], Alessia Serrano[1], Valeria Gerbino[2,3], Alessandra Giorgi[4], Laura Di Francesco[4], Monica Nencini[2], Francesca Bozzo[2,3], Maria Eugenia Schininà[4], Claudia Bagni[5,6,7], Gianluca Cestra[8,9], Maria Teresa Carrì[2,3], Tilmann Achsel[6,7,*] and Mauro Cozzolino[1,2,*]

ABSTRACT

A common feature of non-coding repeat expansion disorders is the accumulation of RNA repeats as RNA foci in the nucleus and/or cytoplasm of affected cells. These RNA foci can be toxic because they sequester RNA-binding proteins, thus affecting various steps of post-transcriptional gene regulation. However, the precise step that is affected by *C9orf72* GGGGCC (G4C2) repeat expansion, the major genetic cause of amyotrophic lateral sclerosis (ALS), is still poorly defined. In this work, we set out to characterise these mechanisms by identifying proteins that bind to *C9orf72* RNA. Sequestration of some of these factors into RNA foci was observed when a $(G4C2)_{31}$ repeat was expressed in NSC34 and HeLa cells. Most notably, $(G4C2)_{31}$ repeats widely affected the distribution of Pur-alpha and its binding partner fragile X mental retardation protein 1 (FMRP, also known as FMR1), which accumulate in intra-cytosolic granules that are positive for stress granules markers. Accordingly, translational repression is induced. Interestingly, this effect is associated with a marked accumulation of poly(A) mRNAs in cell nuclei. Thus, defective trafficking of mRNA, as a consequence of impaired nuclear mRNA export, might affect translation efficiency and contribute to the pathogenesis of *C9orf72* ALS.

KEY WORDS: Amyotrophic lateral sclerosis, C9orf72, Stress granules, mRNA

INTRODUCTION

During the past years, the discovery of mutations in the *FUS* (also known as *TLS*), *TARDBP* and *C9orf72* genes led to the concept that alterations in RNA metabolism are a major determinant of motor neuron degeneration in amyotrophic lateral sclerosis (ALS), similar to what occurs in other neurodegenerative diseases (Walsh et al., 2015). Alterations in alternative splicing have been suggested to cause the disease, but other steps of post-transcriptional gene regulation could be equally involved (Achsel

[1]Institute of Translational Pharmacology, CNR, 00133 Rome, Italy. [2]Laboratory of Neurochemistry, Fondazione Santa Lucia IRCCS, 00143 Rome, Italy. [3]Department of Biology, University of Rome ''Tor Vergata'', 00133 Rome, Italy. [4]Department of Biochemical Sciences ''A. Rossi Fanelli'', University of Rome ''Sapienza'', Rome 00185, Italy. [5]Department of Biomedicine and Prevention, University of Rome ''Tor Vergata'', 00133 Rome, Italy. [6]Center for Human Genetics, KU Leuven, 3000 Leuven, Belgium. [7]VIB Center for the Biology of Disease, 3000 Leuven, Belgium. [8]Institute of Molecular Biology and Pathology, CNR, 00185 Rome, Italy. [9]Department of Biology and Biotechnology ''Charles Darwin'', University of Rome ''Sapienza'', 00185 Rome, Italy.

*Authors for correspondence (Tilmann.Achsel@cme.vib-kuleuven.be; mauro.cozzolino@ift.cnr.it)

et al., 2013). *C9orf72*, the major genetic determinant of ALS (DeJesus-Hernandez et al., 2011; Renton et al., 2011), is a prime example of how little we understand: analogies with other repeat expansion diseases suggest three possible scenarios that could play a role in the pathogenesis of ALS linked to *C9orf72* GGGGCC (G4C2) repeat expansions. One stems from reduced expression of the C9orf72 protein, the others from the accumulation of repeat-containing RNAs that might either trap specific RNA-binding proteins, thereby disrupting RNA processing, or undergo an unconventional mode of translation [repeat-associated non-ATG (RAN) translation], which results in the accumulation of toxic poly-dipeptides (Gendron et al., 2014). However, whether accumulation of toxic RNA species and/or haploinsufficiency of *C9orf72* is the leading pathological mechanism in ALS is unknown.

A common feature of non-coding repeat expansion disorders is the accumulation of RNA repeats as RNA foci in the nucleus and/or cytoplasm of affected cells. These foci are able to sequester RNA-binding proteins, which can affect various steps of post-transcriptional gene regulation, such as alternative mRNA splicing, translational regulation, mRNA transport or mRNA decay (La Spada and Taylor, 2010). In samples from *C9orf72* patients as well as patient-derived induced pluripotent stem cells (iPSCs), RNA foci containing the sense as well the antisense RNA repeat sequence are likewise detected (DeJesus-Hernandez et al., 2011; Donnelly et al., 2013), indicating that the sequestration of RNA-binding proteins and hence a dysregulation in one of the steps of mRNA metabolism might well play a role in ALS. The precise step that is affected, however, remains ill defined, and our understanding of *C9orf72* toxicity thus is still elusive. As a first hint to characterize these mechanisms, we used a biotinylated RNA containing $(G4C2)_{31}$ repeats to identify proteins that bind to *C9orf72* RNA. Based on the ability of $(G4C2)_{31}$ repeats to bind proteins involved in translational control, we analyzed whether protein translation could be affected in cultured cells expressing the same repeats. Indeed, we observed that the expression of $(G4C2)_{31}$ is able to activate a stress response that leads to a general reduction of translation. In these conditions, *C9orf72* repeats strikingly induce an abnormal nuclear accumulation of poly-adenylated mRNAs. Thus, nuclear retention of mRNAs, as a consequence of the ability of the *C9orf72* repeats to impair nuclear mRNA export, might contribute to ALS pathogenesis.

RESULTS

$(G4C2)_{31}$ repeats aggregate in RNA foci in mouse motorneuronal NSC34 cells

In order to produce GGGGCC repeat expansions with selected lengths, we synthesized two complementary oligonucleotides containing three G4C2 repeats and overhangs to allow

1787

head-to-tail ligation. Annealed oligonucleotides were ligated, fractionated on an agarose gel, and various repeat lengths were cloned in an expression vector (pcDNA5/FRT/TO). With this approach, we were able to select a repeat of 31 uninterrupted GGGGCC units $(G4C2)_{31}$ that was transiently transfected into mouse motoneuronal-like NSC34 cells, and compared to a plasmid containing ten repeats $(G4C2)_{10}$. Expression of $(G4C2)_{31}$ was sufficient to induce the appearance of intense intranuclear RNA foci (Fig. 1A), as stained by fluorescence *in situ* hybridization (FISH) analysis using a Cy3-conjugated $(C4G2)_4$ RNA probe. Under the same conditions, ten repeats, whose expression levels are comparable to the $(G4C2)_{31}$ (Fig. 1B), did not form intracellular foci (Fig. 1A). A cytoplasmic staining was also evident in cells transfected with the longer repeat, with cytoplasmic

foci occasionally appearing (Fig. 1A). As expected from the nature of the probe target, treatment with RNase, but not DNase, completely abolished the signal (supplementary material Fig. S1). Transfection of NSC34 cells with a plasmid bearing 270 repeats of the trimer TTC, that is expressed to similar levels as $(G4C2)$ 10 and 31 (Fig. 1B), did not induce the appearance of Cy3-$(C4G2)_4$ positive signals (Fig. 1A). Similarly, a CUG RNA expanded repeat, that is known to form RNA foci, is not recognised by the Cy3-$(C4G2)_4$ probe (supplementary material Fig. S1), further indicating the specificity of the experimental conditions used. The same $(G4C2)_{31}$ repeats were inserted upstream of a GFP coding sequence and transfected in NSC34 cells. As shown in Fig. 1C,D, ~30% of GFP-positive cells showed foci formation after 48 h of transfection, whereas in the same
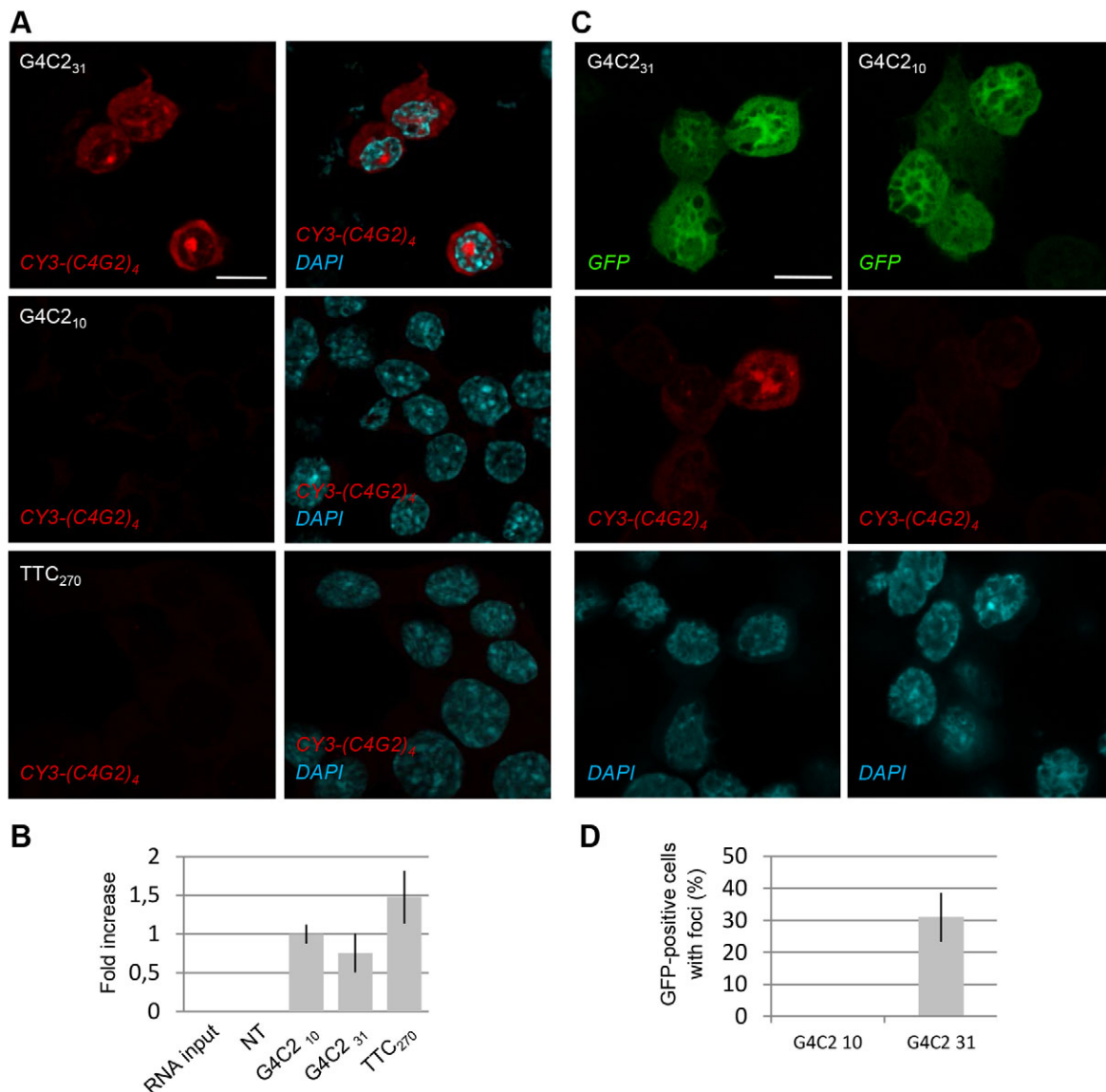

Fig. 1. $(G4C2)_{31}$ repeats form intracellular RNA foci. (A) NSC34 cells were transiently transfected with plasmids coding for 31 (upper panel) or ten (middle panel) G4C2 repeats, and for 270 TTC repeats (lower panel). After 48 h, cells were subjected to FISH analysis with a C4G2 RNA probe conjugated to Cy3 (red). Nuclei were stained with DAPI (blue). Scale bar: 10 μM. (B) Cells were transfected as in A. After 48 h, expression of repeat-containing RNAs was analyzed by RT-qPCR. Shown are the levels relative to the cells expressing the $(G4C2)_{10}$ repeat. RNAs from untransfected cells (NT), as well as input RNAs from $(G4C2)_{31}$-transfected cells (RNA input) were used as the negative control. Mean±s.d. is shown ($n=3$). (C) NSC34 cells were transfected with plasmids coding for $(G4C2)_{31}$ or $(G4C2)_{10}$ repeats and GFP. After 48 h, cells were subjected to FISH analysis with a Cy3–C4G2 RNA probe. Nuclei were stained with DAPI (blue). Scale bar: 10 μm. (D) The percentage of GFP-expressing cells that show RNA foci was scored (mean±s.d. from $n=3$ independent experiments).

conditions of GFP expression, no foci are detectable in cells transfected with a GFP-(G4C2)$_{10}$ plasmid. Therefore, the accumulation into nuclear foci is a prevalent feature of (G4C2)$_{31}$ RNA repeat expression. Further, overexpression of 31 repeats is sufficient to reproduce a key pathological phenotype that characterizes *C9orf72* patients carrying longer expansions.

Repeat-binding proteins are involved in pre-mRNA splicing and mRNA translation

To get insights into the mechanisms whereby *C9orf72* might induce cell toxicity, we used an *in-vitro*-transcribed biotinylated RNA containing the (G4C2)$_{31}$ repeats to affinity purify proteins able to bind it. The major repeat-binding proteins from mouse brain and spinal cord extracts were visualised by Coomassie staining of SDS-polyacrylamide gels, excised and identified by mass spectrometry (supplementary material Table S1; Fig. S2). Among the interactors, we found different factors involved in post-transcriptional gene regulation. Indeed, G4C2-repeat-binding proteins are enriched in members of the heterogeneous nuclear ribonucleoprotein (hnRNP) family (hnRNP H, hnRNP U, hnRNP Q), which are known key regulators of alternative splicing (Chen and Manley, 2009). However, translational regulators also bind (G4C2)$_{31}$: these include initiation and elongation factors (EF1α,

eIF2α, eIF2β and eIF2γ), and also Pur-alpha (Pura), Pur-beta and other translation regulatory proteins [ILF2, ILF3 and RAX (also known as PRKRA or PACT)]. To validate the mass spectrometry data, a subset of the identified proteins was analyzed by western blotting on proteins pulled down by the (G4C2)$_{31}$ RNA repeat from mouse brain and spinal cord (data not shown), as well as mouse (NSC34) and human (SH-SY5Y) cultured neuronal cells. As shown in Fig. 2A, all the proteins tested could be detected, with different binding affinity depending on the stringency conditions. When the same proteins were analyzed in extracts pulled down with a biotinylated (TTC)$_{270}$ RNA repeat, only hnRNP H, eIF2α, eIF2β and RAX displayed a significant specificity for the (G4C2)$_{31}$ RNA repeat, whereas the other proteins tested precipitate to the same or even higher degrees (Fig. 2B,C). By contrast, none of the proteins tested was detected in control precipitates. Overall, these data suggest that G4C2 binding to Pura, hnRNP U, ILF2 and ILF3 might not be required for *C9orf72* toxicity. Based on their described ability to bind the *C9orf72* repeats (Lee et al., 2013; Mori et al., 2013; Reddy et al., 2013), we also checked for the presence of FUS, TDP43, hnRNPA2/B1 and SRSF1 as repeat-binding partners (Fig. 2D). Again, binding of these proteins to (G4C2)$_{31}$ was observed. Importantly, MBNL1, whose sequestration by CUG RNA repeats has a prominent role in DM1 pathogenesis, was in no
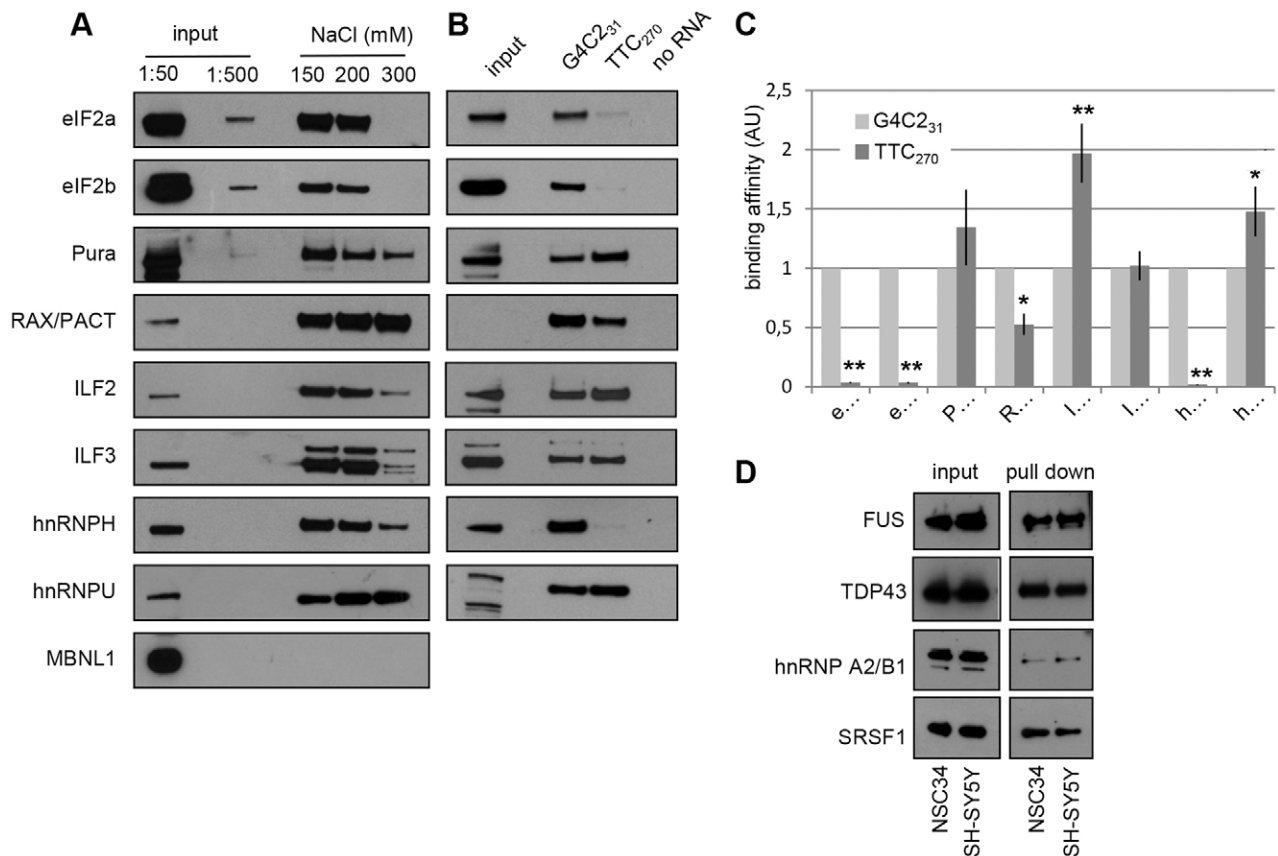

Fig. 2. (G4C2)$_{31}$ repeat RNA binds factors involved in pre-mRNA splicing and mRNA translation. (A) Lysates from NSC34 cells were incubated at the indicated NaCl concentrations with a biotinylated (G4C2)$_{31}$ repeat. Pulled-down proteins were then analyzed by western blotting with the indicated antibodies. 0.2% and 2% of inputs were analyzed as a loading control. The two different ILF3 isoforms of 90 and 110 kDa are bound. (B) Lysates from NSC34 cells were incubated at 200 mM NaCl concentration in the absence (no RNA) or in the presence of biotinylated (G4C2)$_{31}$ or (TTC)$_{270}$ repeats, and analyzed by western blotting as indicated. 2% of inputs were analyzed as a loading control. (C) Quantification of the precipitation efficiency shown in B. The amounts of the indicated proteins are expressed as mean±s.d. of arbitrary densitometric units (AU) relative to (G4C2)$_{31}$ precipitates. *$P<0.05$, **$P<0.01$ compared with relative controls ($n=3$). (D) Lysates from NSC34 or SH-SY5Y cells were incubated with biotinylated (G4C2)$_{31}$ RNA and pulled-down proteins were analyzed by western blotting with indicated antibodies.

instance precipitated by *C9orf72* repeats (Fig. 2A), indicating that $(G4C2)_{31}$ repeat is selective for the binding to a subset of RNA binding proteins.

$(G4C2)_{31}$ repeats sequester RBPs into RNA foci and disturb the intracellular localization of Pura and FMRP

Sequestration of $(G4C2)_{31}$-binding proteins into RNA foci has been suggested to cause a decreased availability of those proteins, thus affecting their function and eventually leading to cell death. We therefore looked for the presence of the above identified proteins in RNA foci formed by $(G4C2)_{31}$ repeats in NSC34 cells. Among the proteins tested, hnRNP H, eIF2α, FUS and ILF3 showed a clear colocalization with RNA foci (Fig. 3A), whereas the other proteins did not significantly colocalize (not shown). To assess whether the accumulation of $(G4C2)_{31}$-binding proteins into RNA foci could be dependent on the cellular context, we also performed a similar analysis in human HeLa cells, obtaining comparable results (Fig. 3B). In both cellular types, however, the number of cells where RNA foci colocalized with those proteins was extremely low (less than 3%). Thus, although the presence of the proteins into RNA foci indicates that their interaction with G4C2 repeats also occurs *in vivo*, these results suggest that the formation of RNA foci by the $(G4C2)_{31}$ repeats does not normally affect the overall subcellular distribution of the partners analyzed. Pura represents a striking exception. Indeed, whereas this protein only occasionally showed a clear colocalization with RNA foci, in almost all the cells displaying $(G4C2)_{31}$ RNA foci formation, the intracellular distribution of Pura was profoundly affected, with an evenly diffused localization in the cytosol of untransfected cells, but with it coalescing into cytosolic and nuclear granules in cells with RNA foci. A similar result was obtained with FMRP, a known binding partner of Pura (Fig. 4A). In cells transfected with $(G4C2)_{31}$ repeats, FMRP accumulated into cytosolic and, to a lesser extent, nuclear granules. The same pattern of Pura and FMRP delocalization was induced by $(G4C2)_{31}$ expression in HeLa cells (Fig. 4B). Interestingly, FMRP is also pulled down by $(G4C2)_{31}$ RNA (supplementary material Fig. S3), but differently from other partners analyzed, this interaction was completely lost when the NaCl concentration was raised to 300 mM, suggesting that the binding of FMRP is not direct, and might be mediated by Pura itself. This conclusion is further supported by the observation that Pura and FMRP colocalized in cells expressing the $(G4C2)_{31}$ repeats, but not the $(G4C2)_{10}$ nor the $(TTC)_{270}$ repeats (supplementary material Fig. S3).

$(G4C2)_{31}$ repeats induce translational arrest

The ability of $(G4C2)_{31}$ repeats to bind eIF2α, a central controller of protein translation, as well as the effects of repeat expression on the subcellular distribution of Pura and FMRP, whose functions in protein translation are well documented (Bagni and Oostra, 2013; White et al., 2009), prompted us to analyze whether $(G4C2)_{31}$ is able to affect protein translation. HeLa cells, a well established model to study stress response, were therefore transiently transfected with $(G4C2)_{31}$ repeats, and the presence of stress granules, where non-functional translation initiation complexes accumulate in response to stress, was analyzed. Indeed, stress granules were formed in the vast majority of cells expressing the $(G4C2)_{31}$ repeats, but not in cells expressing similar amounts of $(G4C2)_{10}$ or $(TTC)_{270}$ RNAs, as measured by the presence of intra-cytoplasmic granules that are positive for TIA-1-related protein (TIAR, also known as TIAL1), a known stress granule marker (Fig. 5A–D). Importantly, Pura granules

(Fig. 5A), as well as FMRP granules (data not shown), are positive for TIAR. Thus, *C9orf72* repeat is able to activate in cells a stress response that induces stress granules formation.

Phosphorylation of eIF2α (P-eIF2α) is the leading mechanism that causes the formation of non-functional translation initiation complexes and their accumulation into stress granules, and the phosphorylation status of eIF2α is thus an indication of translational inhibition (Spriggs et al., 2010). P-eIF2α levels were therefore monitored with a phospho-specific antibody in HeLa cells transfected with $(G4C2)_{31}$ repeats. As shown in Fig. 6A, no significant increase in eIF2α phosphorylation was detectable in cells expressing the $(G4C2)_{31}$ repeats, compared to cells expressing shorter expansions (ten repeats) or to mock-transfected cells. By contrast, in the same cells treated with thapsigargin, a well-known inducer of ER stress mediated through the activation of PERK kinase (also known as EIF2AK3), a significant increase in P-eIF2α was detected. Thus, eIF2α phosphorylation does not seem to be a crucial step in the stress response induced by $(G4C2)_{31}$.

To check whether this response is nonetheless sufficient to cause translation inhibition, cells were analyzed for their ability to incorporate puromycin into nascent polypeptides as a measure of the rate of mRNA translation (Schmidt et al., 2009). Both western blot analysis (Fig. 6B) and immunofluorescence staining (Fig. 6C,D) of transfected cells clearly shows that puromycin incorporation is considerably decreased in HeLa and NSC34 cells expressing $(G4C2)_{31}$, but not $(G4C2)_{10}$ nor $(TTC)_{270}$ repeats. As expected, pre-treating of cells with cycloheximide completely abolishes puromycin incorporation.

mRNAs accumulate in nuclei of $(G4C2)_{31}$-expressing cells

Previous data indicate that a significant inhibition of global mRNA translation is achieved in cells expressing *C9orf72* repeats independently from the phosphorylation of eIF2α, thus implying alternative mechanisms whereby translational inhibition is carried out by G4C2 expansions. One obvious possibility is that G4C2 RNA repeats might cause a failure in mRNA export from nuclei, eventually leading to the accumulation of poly(A) RNAs into them. To investigate this possibility, cells were left untransfected or were transfected with $(G4C2)_{10}$ or $(G4C2)_{31}$ repeats, and poly(A) RNAs were visualized by oligo(dT) FISH. To exclude the possibility that the probe might recognize the poly(A) tail of the overexpressed $(G4C2)_{31}$ RNAs that indeed accumulate in nuclei, the repeat sequence was cloned under the control of an RNA polymerase III promoter, and a small poly(T) stretch was inserted immediately after the repeat sequence as a transcription termination signal. As shown in Fig. 7A–C, an enhancement of the poly(A) RNA signal in the nucleus was clearly detectable in cells displaying G4C2 RNA foci, compared to untransfected or $(G4C2)_{10}$-transfected cells (supplementary material Fig. S4A). Importantly, poly(A) RNAs accumulate as nuclear dots that only partially colocalize with $(G4C2)_{31}$ RNA foci, thus excluding a direct sequestration of poly(A) mRNAs by the repeat sequence. When stress granule formation was induced by sodium arsenite, poly(A) mRNAs aggregated in TIAR-positive stress granules, as expected (Fig. 7D). In this condition, however, no mRNA accumulation in cell nuclei was observed, suggesting that nuclear mRNA retention by the $(G4C2)_{31}$ repeat is not a mere consequence of the formation of cytoplasmic stress granules. This conclusion is further supported by the subcellular distribution of the cytoplasmic poly(A)-binding protein (PABPc, also known as PABPC1) in cells expressing $(G4C2)_{31}$ repeats. It has been recently shown, in fact, that nuclear accumulation of poly(A)
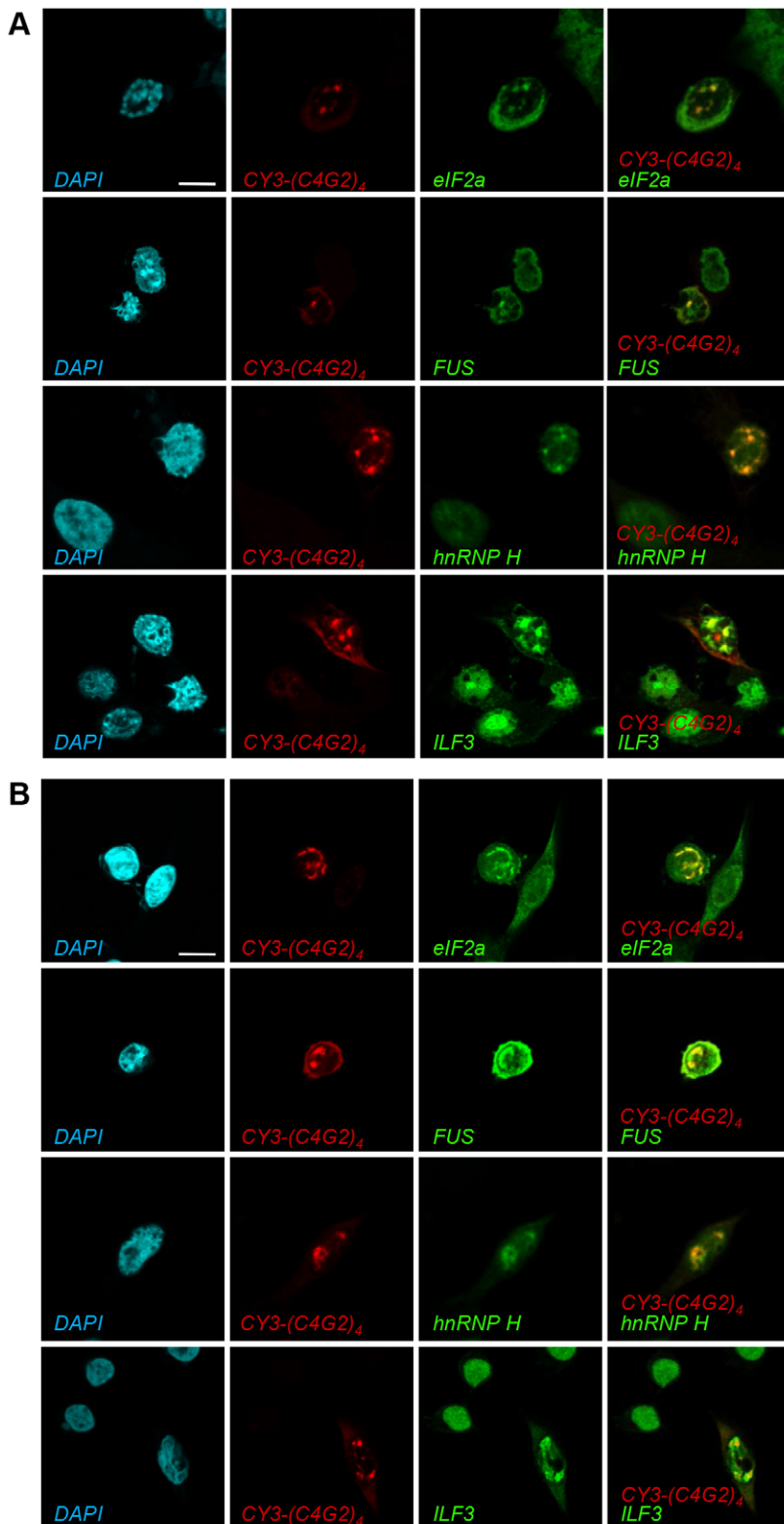
Fig. 3. (G4C2)₃₁ repeats sequester RNA-binding proteins into RNA foci. (A) NSC34 cells were transiently transfected with a plasmid expressing (G4C2)₃₁ repeats and analyzed after 48 h by RNA FISH using a Cy3–(C4G2)₄ probe (red) and by immunofluorescence staining (green) with antibodies recognizing different RNA-repeat-binding proteins (eIF2α, FUS, hnRNP H and ILF3). (B) HeLa cells were transiently transfected with a plasmid expressing (G4C2)₃₁ repeats and analyzed after 24 h as in A. The overlay of the two colors is shown. Nuclei were stained with DAPI. Scale bars: 10 μm.

RNAs is associated with relocalization of PABPc in cell nuclei. PABPc has an established, fundamental role in cytosolic mRNA translation and stability (Burgess et al., 2011; Kumar and Glaunsinger, 2010) and it is known to localize into stress granules upon stress (Kedersha et al., 2000). We therefore analyzed PABPc distribution in cells expressing the (G4C2)₃₁

repeats. Immunofluorescence staining of cells shows that, as expected, PABPc has a prevalent cytoplasmic steady-state localization in a majority of untransfected cells. However, in a substantial fraction of (G4C2)₃₁-transfected cells (10±2%, ±s.d.), an evident nuclear PABPc signal could be seen (Fig. 8A), whereas the cytosolic distribution of PABPc in cells expressing (G4C2)₁₀ or

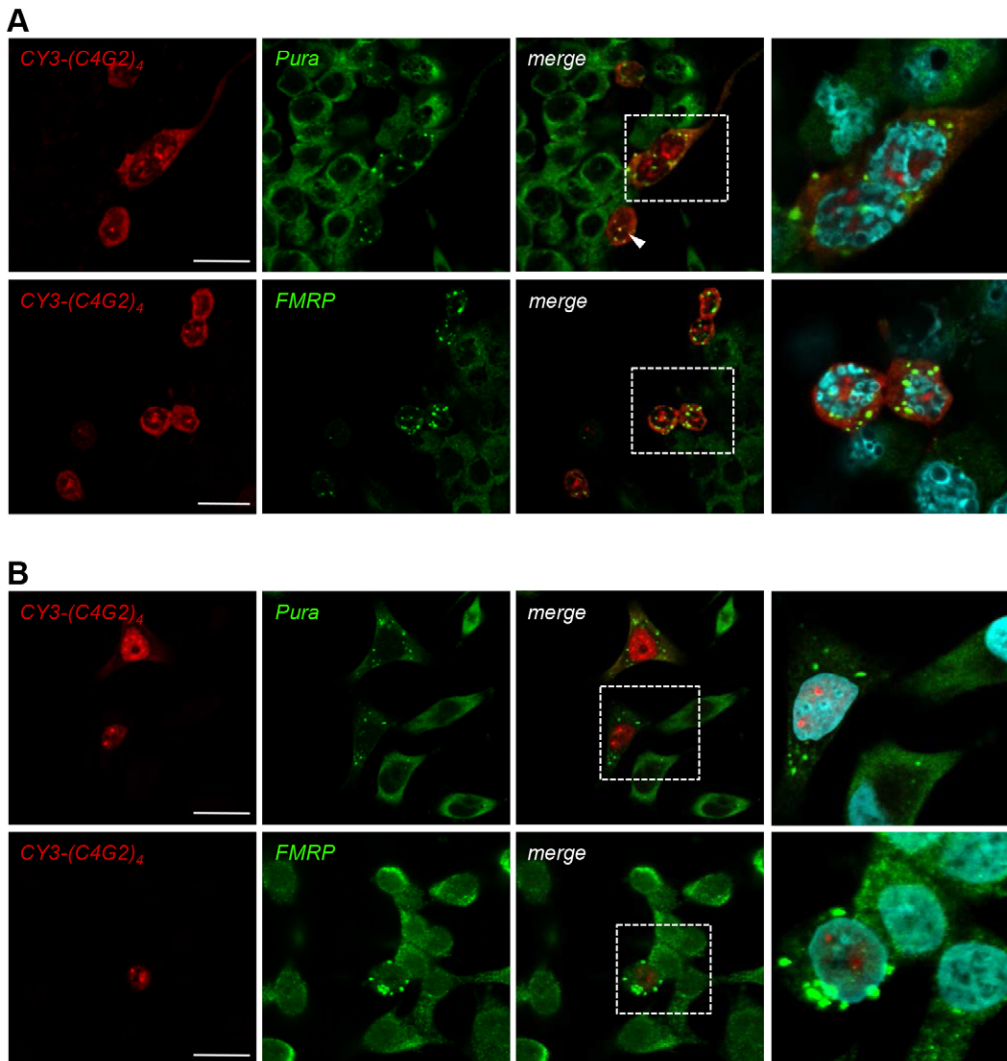**Fig. 4. (G4C2)$_{31}$ repeats affect Pura and FMRP localization in NSC34 and HeLa cells.** (A) NSC34 cells were transiently transfected with a (G4C2)$_{31}$-expressing plasmid and analyzed after 48 h by RNA FISH using a (C4G2)$_4$ probe conjugated to Cy3 (red) and by immunofluorescence staining (green) with anti-Pura (upper panels) and anti-FMRP (lower panels) antibodies. In untransfected cells, Pura and FMRP have a diffuse cytosolic localization, whereas in cells that express (G4C2)$_{31}$ repeats both proteins accumulate into cytosolic and nuclear granules. The white arrowhead points to a nuclear granule where Pura and G4C2 repeat colocalise. Higher magnifications of the areas highlighted by the box are shown together with DAPI staining. (B) HeLa cells were transiently transfected with (G4C2)$_{31}$ repeats and analyzed after 24 h by RNA FISH as in A. Scale bars: 20 μm.

(TTC)$_{270}$ was unaffected (Fig. 8B) A similar result was obtained when cells were transfected with repeat-GFP plasmids (supplementary material Fig. S4B), or when nuclear and cytoplasmic fractions of cells were analyzed by western blotting (Fig. 8C). Interestingly, a considerable number of transfected cells displayed a clear accumulation of PABPc into RNA foci (Fig. 8A), and PABPc is pulled down by (G4C2)$_{31}$ RNA (Fig. 8D), but not by (TTC)$_{270}$ RNA. Importantly, PABPc only rarely colocalized with the Pura-containing cytosolic stress granules that were induced by (G4C2)$_{31}$ repeats, which is different from what is observed in cells treated with arsenite, where PABPc and Pura fully colocalize (Fig. 8E). Thus, a nuclear relocalization of PABPc is specifically induced by (G4C2)$_{31}$, and this is associated with the nuclear retention of poly(A) mRNAs.

DISCUSSION

The presence of *C9orf72* RNA inclusions in tissues from ALS or frontotemporal dementia (FTD) patients, as well as the formation of similar inclusions in cellular systems expressing the repeats, including iPSC-derived motor neurons, provided an early support for the hypothesis that sequestration of RNA-binding proteins by *C9orf72* repeat might have a role in disease pathogenesis (Walsh et al., 2015). Evidence from histopathological analysis of RNA foci in tissues from ALS and/or FTD patients has shown a

positive correlation between the number of repeat-containing foci and disease presentation or severity (Cooper-Knock et al., 2014; Mizielinska et al., 2013), further indicating that accumulation of *C9orf72*-derived G4C2 RNA repeats are primary involved in the neurodegenerative process. However, the nature of the mechanisms affected by this accumulation is still unknown. To get insights into this process, we have characterized the major binding partners of a (G4C2)$_{31}$ repeat. Our analysis showed that a substantial number of binding partners are RNA regulatory factors, as expected by the nature of the repeat sequence and in line with previous analyses showing that splicing and translation regulatory factors are binding partners of *C9orf72* (Cooper-Knock et al., 2014; Donnelly et al., 2013; Haeusler et al., 2014; Mori et al., 2013; Xu et al., 2013). In our study, translational regulators are particularly represented: these include initiation and elongation factors (EF1α, eIF2α, eIF2β, eIF2γ), but also Pura, Pur-beta and other translation regulatory proteins (ILF2, ILF3 and RAX). Trying to figure out which of these interactors might be more directly involved in *C9orf72* repeat toxicity, we therefore reasoned that the amount of sequestration into RNA foci might represent a discriminating factor. Surprisingly, at least among the binding partners tested, only a limited number were found in association with the RNA foci that are formed in cultured cells by the expression of 31 repeats, and even in these
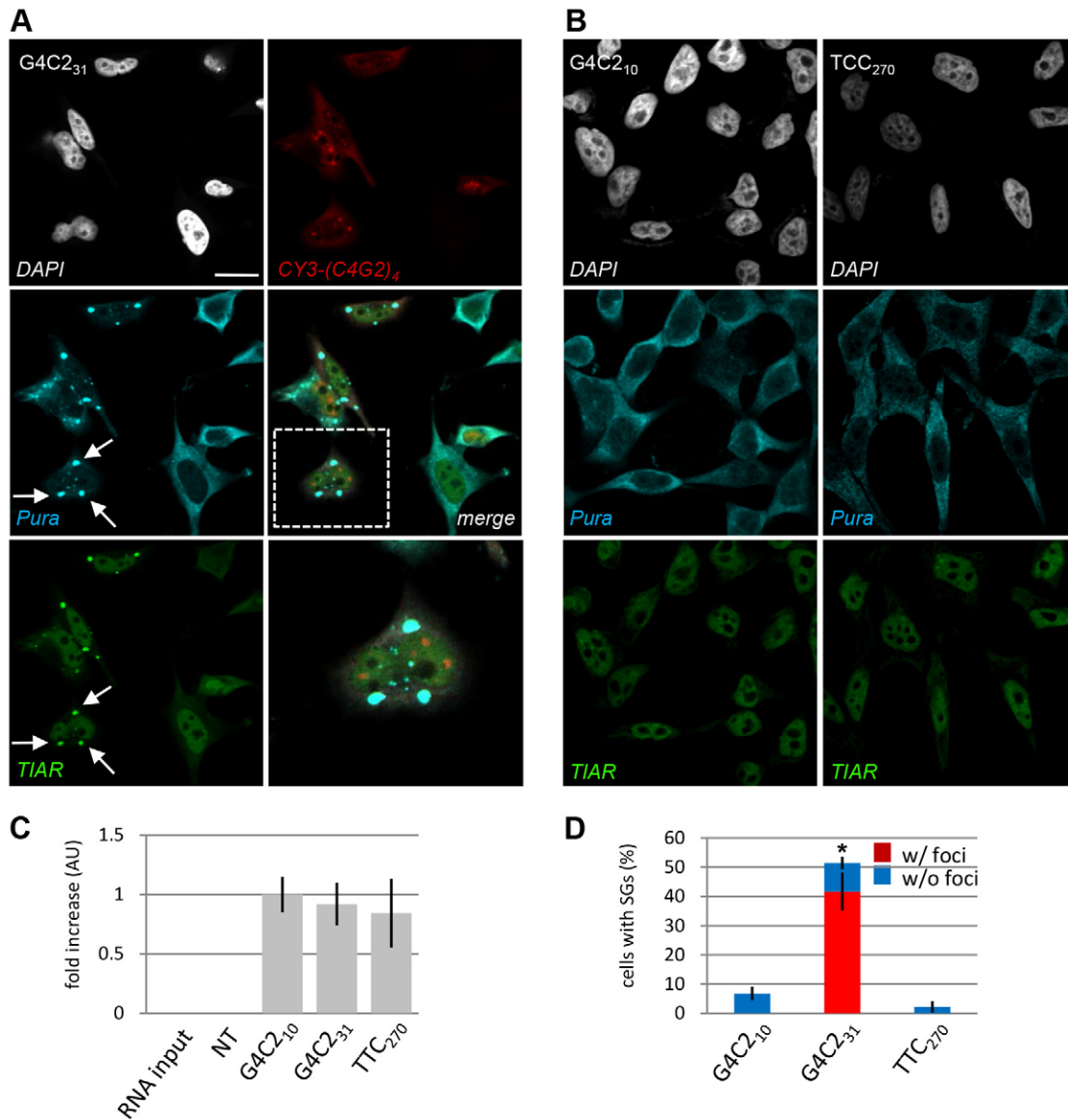
Fig. 5. (G4C2)₃₁ repeats induce stress granules formation. (A) HeLa cells were transiently transfected with a plasmid expressing (G4C2)$_{31}$ repeats. After 24 h, RNA foci were visualized by FISH analysis with a Cy3–(C4G2)$_4$ probe conjugated to Cy3 (red) together with immunofluorescence staining with anti-TIAR (green) and anti-Pura (blue) antibodies. The overlay of the three colors (merge), and a higher magnification of the area highlighted by the box are shown. In cells expressing (G4C2)$_{31}$ repeats, Pura accumulates in TIAR-positive stress granules (white arrows). Nuclei were stained with DAPI (white). Scale bar: 20 µm. (B) HeLa cells were transfected with (G4C2)$_{10}$ or (TTC)$_{270}$ plasmids as in A. After 24 h, immunofluorescence staining with antibodies anti-TIAR (green) and anti-Pura (blue) was performed, together with DAPI staining (white). Images are presented at the same magnification as in A. (C) Cells were transfected as in A with the indicated plasmids. After 24 h, expression of repeat-containing RNAs was analyzed by qRT-PCR. Shown are the levels relative to the cells expressing the (G4C2)$_{10}$ repeat. RNAs from untransfected cells, as well as input RNAs from (G4C2)$_{31}$-transfected cells were used as negative control. Mean±s.d. is shown (n=3). (D) Cells transfected with the indicated plasmids and presenting stress granules were scored and plotted according to the presence (w/, with foci, red) or absence (w/o, without foci, blue) of RNA foci. Values are reported as mean percentage ± s.d. from three independent experiments. *P<0.01 compared with relative controls.

cases, the amount of colocalization was really low (supplementary material Table S2). Clearly, we cannot exclude that the length of the repeats, as well as the duration of the process, can influence the appearance of such a phenotype. Indeed, observations in brain tissues from *C9orf72* ALS and FTD patients, who usually bear longer expansions that accumulate over a large period of time, show that a substantial number of G4C2 RNA foci colocalize with hnRNP H (Lee et al., 2013), and to a lower, but still significant extent, with SRSF2 and ALYREF (Cooper-Knock et al., 2014). This argues in favor of such a

conclusion. However, numerous inconsistencies emerge from studies where tissues from ALS and/or FTD patients have been surveyed for proteins that co-aggregate with RNA foci (Stepto et al., 2014), suggesting that a dynamic interaction between accumulated RNA repeats, either aggregated in foci or not, and selected targets, rather than an irreversible sequestration, might better describe the pathogenic mechanism (Cooper-Knock et al., 2014). Our results support this idea and suggest that RNA repeats might affect the proper localization and/or function of a distinguished set of RNA-binding proteins independently from
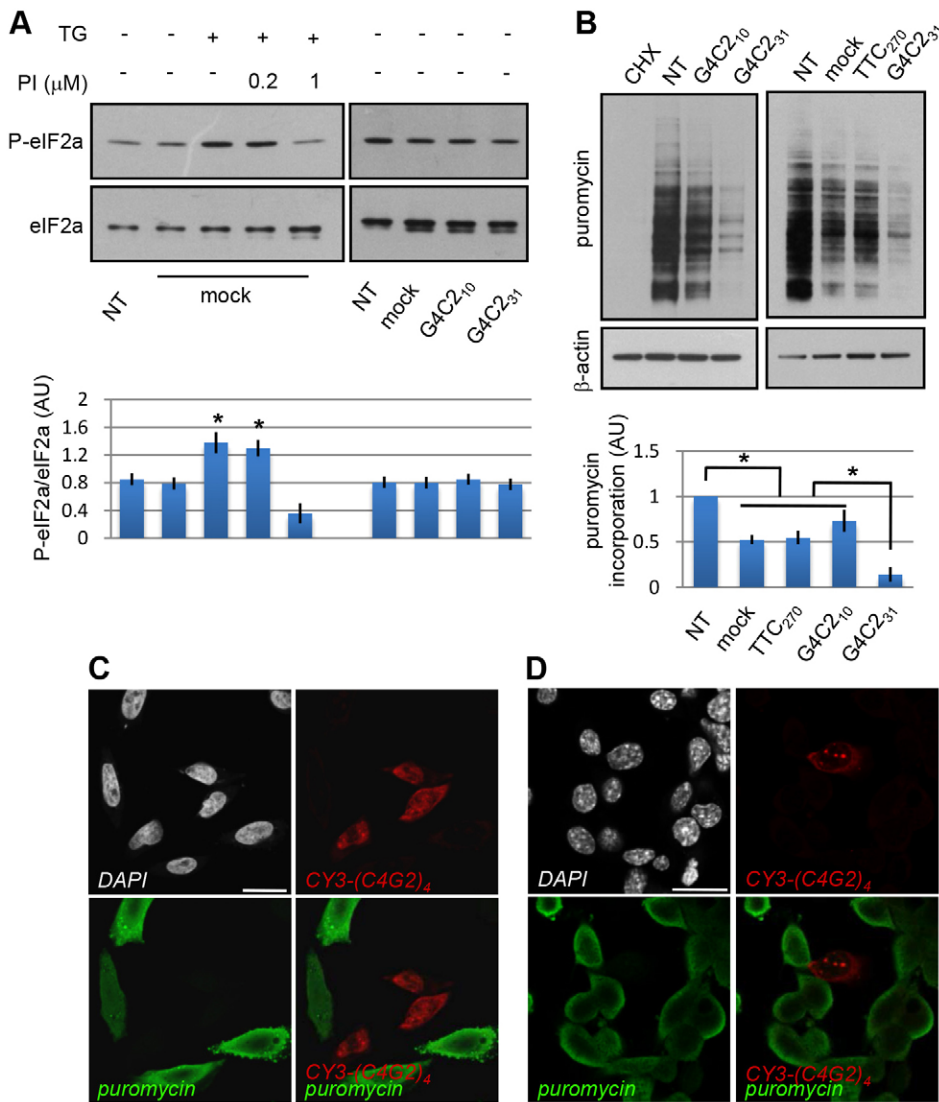
Fig. 6. (G4C2)$_{31}$ repeats induce eIF2α-phosphorylation-independent translational arrest. (A) Untransfected HeLa cells or cells transiently transfected with mock, (G4C2)$_{10}$ or (G4C2)$_{31}$ plasmids, were grown in the absence or presence of the PERK inhibitor GSK2606414 (PI), at the indicated concentrations. After 24 h, where specified, cells were treated with 5 µM thapsigargin (TG) for 2 h, and cell lysates were analyzed by western blotting with antibodies that specifically recognize phosphorylated eIF2α (P-eIF2a) or total eIF2α. The lower panel shows the quantification of the bands, presented as the ratio of the P-eIF2α over the total eIF2α and expressed in arbitrary units (AU), and reported as mean±s.d.; $n=4$. *$P<0.01$ compared with relative controls. (B) HeLa cells were left untransfected (NT), or were transiently transfected with an empty vector (mock), or vectors containing (G4C2)$_{10}$, (G4C2)$_{31}$ and (TTC)$_{270}$ repeats. After 24 h, cells were treated with 10 µg/ml puromycin for 10 min and cell lysates were analyzed by western blotting with an antibody against puromycin. β-actin was analyzed as a standard for equal protein loading. The puromycin incorporation rate in untransfected cells pre-treated with 1 mM cycloheximide (CHX) for 10 min was also analyzed. The lower panel shows the quantification of the bands, expressed in arbitrary units (AU), relative to untransfected cells, and reported as mean±s.d.; $n=3$. *$P<0.01$ compared with relative controls. (C) HeLa cells were transiently transfected with a plasmid expressing (G4C2)$_{31}$ repeats. After 24 h, cells were treated with puromycin, and then analyzed by Cy3–(C4G2)$_4$ RNA FISH (red) and by immunofluorescence staining with an anti-puromycin antibody (green). Nuclei were stained with DAPI (white). (D) NSC34 cells were transiently transfected with (G4C2)$_{31}$ repeats, and analyzed as in (C) after 48 h. Scale bars: 20 µm.

their sequestration into nuclear foci, a conclusion that is also consistent with the presence of RNA repeats in the cytosol of cells, where they do not necessarily form RNA inclusions containing co-aggregated proteins. Among these RNA binding proteins, hnRNPH, eIF2α, eIF2β and RAX might represent relevant targets of C9orf72 expansion, as their interaction with the (G4C2)$_{31}$ repeat proved to be specific when compared to the binding to an unrelated TTC repeat expansion that is not sufficient to induce cellular phenotypes when expressed in NSC34 or HeLa cells. However, Pura, which has been implicated in G4C2-induced neurodegeneration (Xu et al., 2013), binds to the two repeats with the same affinity. Thus, the nature of the particular RNA process affected by *C9orf72* could not be easily anticipated by a colocalization analysis or simply argued by the types of binding partners found to be associated to the repeats, and a functional analysis is needed to draw any conclusion.

Functionally, the most striking effect of *C9orf72* expression is the induction of translational arrest. Indeed, in this study we show for the first time that stress granules are formed in cells where *C9orf72* RNA repeats accumulate into nuclear foci, and this phenotype well correlates with a strong reduction in the rate of global translation. Mounting evidence indicates that stress-granule-associated translational repression might have a role in ALS pathogenesis. FUS and TAR DNA-binding protein 43 (TDP-43, also known as TARDBP), two major ALS factors, are known to accumulate into stress granules upon stress, and ALS-linked mutations clearly affect stress granule formation, eventually impairing a neuroprotective effect of this process or generating a persistent presence of stress that might be harmful to neurons (Bentmann et al., 2013). Moreover, stress granule genes are potent modifiers of TDP-43 toxicity in *Drosophila*, and decreased translational repression has a protective effect (Kim et al., 2014). Thus, our observations extend this scenario to *C9orf72*-mediated ALS. In the cell lines tested, however, phosphorylation of eIF2α, which results in decreased production of the ternary complex needed for translation initiation, does not seem the major mechanism whereby translational inhibition is achieved. Based on the interaction between the G4C2 RNA repeat and eIF2α, which we found occurred both *in vitro* and in cell culture, it could be assumed that eIF2α function might be impaired independently from its phosphorylation, and that this might in turn be responsible for the observed assembly of stress granules. Indeed, stress
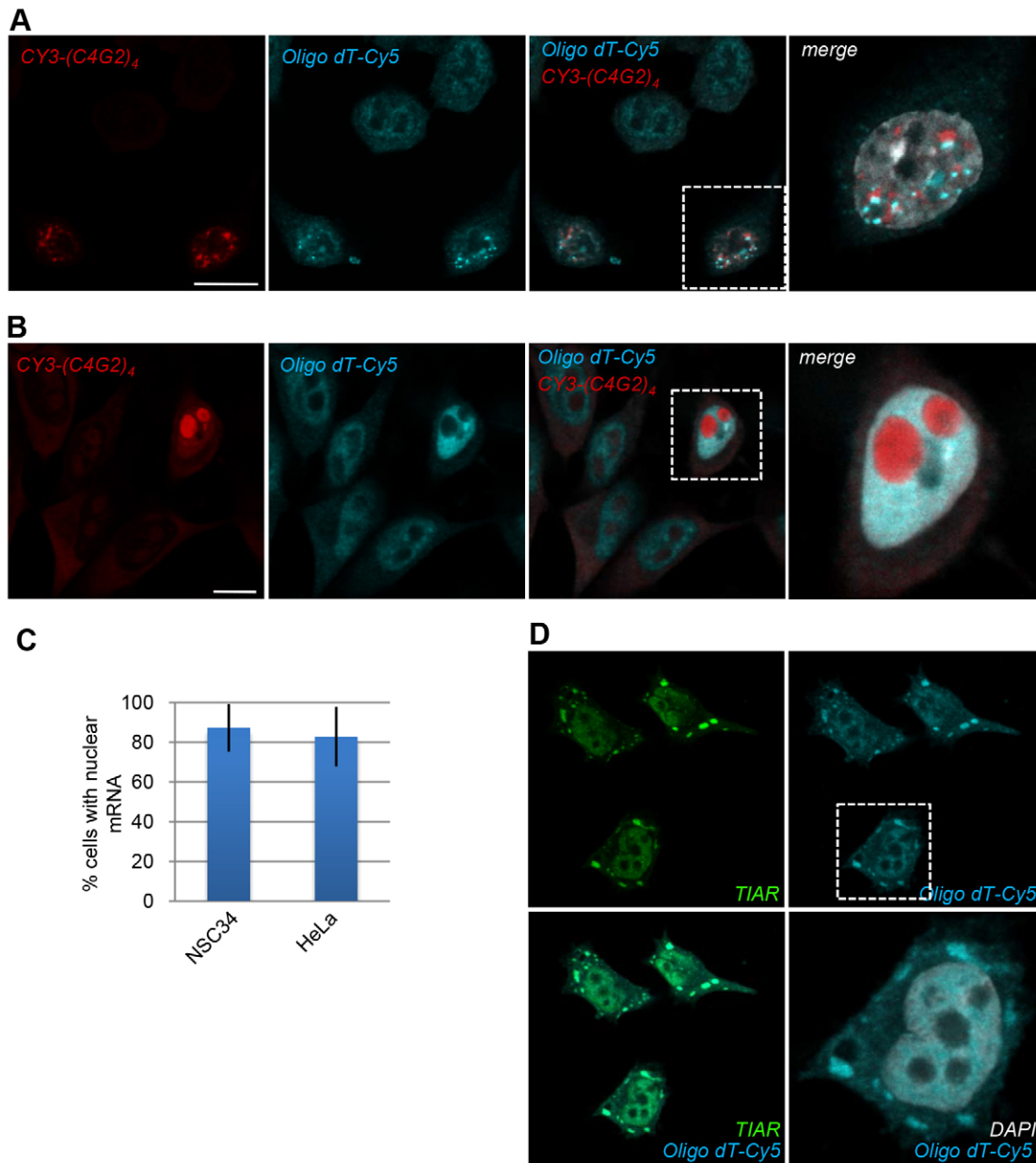
Fig. 7. mRNAs accumulate in the nuclei of cells expressing (G4C2)$_{31}$ repeats. (A) NSC34 cells were transiently transfected with a plasmid (pSUPER.retro.puro) expressing (G4C2)$_{31}$ repeats and analyzed after 48 h by RNA FISH using a (C4G2)$_4$ probe conjugated to Cy3 (red) and an oligo(dT) probe labeled with Cy5 (blue). Scale bar: 20 µm. (B) HeLa cells were transfected and analyzed after 24 h as in (A). In cells expressing (G4C2)$_{31}$ repeats mRNAs accumulate as nuclear dots, that partially colocalize with RNA foci. A higher magnification of the areas highlighted in the inset is shown, together with DAPI staining (grey). Scale bar: 10 µm. (C) Cells presenting RNA foci were scored and plotted according to the presence of mRNA accumulated in nuclei. At least 50 cells for each condition were counted. Values are reported as the mean percentage ± s.d. from three independent experiments. (D) HeLa cells were treated with 1 mM NaAs for 30 min and analyzed by RNA FISH using an oligo(dT) labeled with Cy5 (blue). Cells were also stained with an anti-TIAR antibody (green). A higher magnification of the area highlighted in the inset is shown, together with DAPI staining (white). Images in D are presented at the same magnification as in B.

granules are formed when the availability of eIF2α, as well as other translational factors, is decreased by small interfering RNA (siRNA) (Mokas et al., 2009), a situation that might be mimicked by RNA repeat sequestration. As an alternative, decreased mRNA export from cell nuclei, as suggested by the clear accumulation of poly(A) RNA in the nuclei of cells expressing (G4C2)$_{31}$ repeats, might explain, at least in part, this phenomenon. Which is the factor that provokes nuclear accumulation of poly(A) mRNAs in the presence of G4C2 RNA

expression? One interesting possibility is that nuclear accumulation of PABPc might be the principal driver of mRNA nuclear retention. The cytoplasmic form of PABP (PABPc) is a nucleo-cytosol shuttling protein with a steady-state expression in the cytoplasm, where it enhances translational efficiency by bridging the poly(A) tail to the cap-binding complex through the eIF4G protein (Smith et al., 2014). Further, PABPc is found into stress granules upon cell stress (Kedersha et al., 2000). However, PABPc is also known to relocalize in the nuclei of cells when
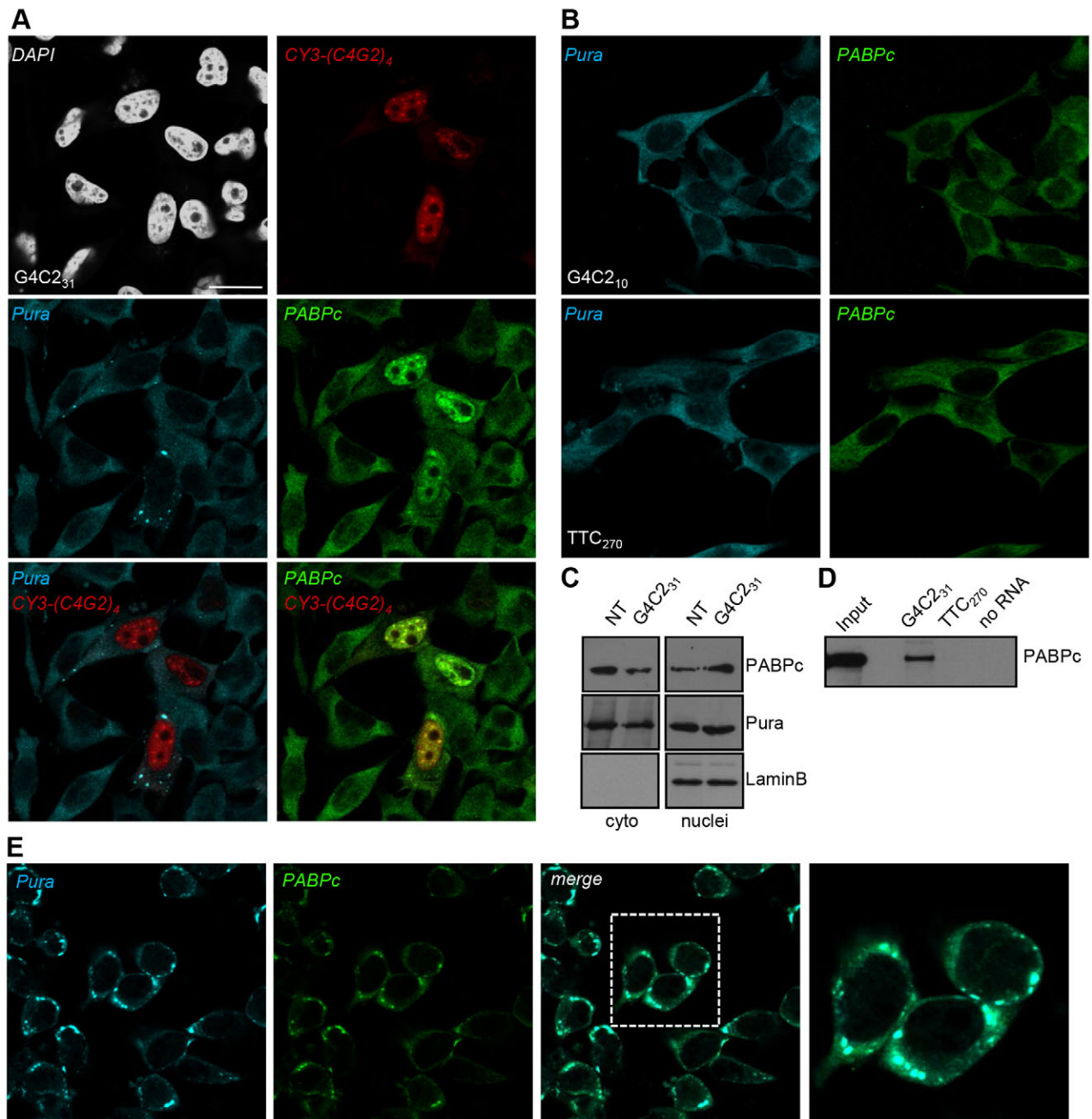
Fig. 8. (G4C2)$_{31}$ repeats induce the re-localization of cytoplasmic PABP in cell nuclei. (A) HeLa cells were transiently transfected with (G4C2)$_{31}$ repeats and analyzed after 24 h by RNA FISH (red) and by immunofluorescence staining with anti-PABPc (green) and anti-Pura (blue) antibodies. Nuclei were stained with DAPI (white). Scale bar: 20 µm. (B) HeLa cells were transfected with (G4C2)$_{10}$ or (TTC)$_{270}$ plasmids and stained after 24 h with anti-PABPc (green) and anti-Pura (blue) antibodies (C) HeLa cells were transiently transfected with (G4C2)$_{31}$ repeats or left untransfected (NT). After 24 h, nuclear and cytosolic fractions from cells were isolated and analyzed by western blotting using an anti-PABPc antibody. Pura and the nuclear protein lamin B were also examined as standards for equal protein loading in the two fractions. (D) Lysates from HeLa cells were incubated with NaCl (200 mM) in the absence (no RNA) or in the presence of biotinylated (G4C2)$_{31}$ or (TTC)$_{270}$ repeats, and analyzed by western blotting with an anti-PABPc antibody. 0.5% input was analyzed as a loading control. (E) HeLa cells were treated with 1 mM NaAs for 30 min and analyzed by immunofluorescence staining with anti-PABPc (green) and anti-Pura (blue) antibodies. A higher magnification of the highlighted area is shown. Images in B and E are presented at the same magnification as in A.

accumulation of mRNAs in cell nuclei as well as translational inhibition are induced by a subset of viral proteins (Smith and Gray, 2010). Interestingly, the obligatory expression of a nuclear targeted PABPc protein is sufficient to cause a dramatic increase in poly(A) mRNAs in cell nuclei (Kumar and Glaunsinger, 2010). Thus, PABPc localization appears to be an important determinant

of mRNA fate. We observed in this work that *C9orf72* G4C2 repeats bind to PABPc, sequester it into nuclear foci and induce its nuclear accumulation. For these reasons, it is tempting to speculate that nuclear retention of PABPc by G4C2 might represent a crucial point in the pathogenic cascade that originates from RNA repeat expression, and could be in accordance with the evidence showing

that PABPc is found in TDP43-containing inclusions in ALS patients (McGurk et al., 2014). This suggests that PABPc could be an important factor in the pathology of ALS. However, nuclear accumulation of PABPc might be one required component of the observed phenomena, but other factors might be necessary as well. Among the *C9orf72*-binding partners, the mRNA export adaptor ALYREF has been recently described to be highly represented in RNA foci in cerebellar granule cells and in motor neurons from *C9orf72* ALS patients (Cooper-Knock et al., 2014). This observation suggests that accumulated RNA repeats might interfere with the proper delivery of mRNAs from nuclei to cytosol, eventually affecting gene expression. As a matter of fact, Fragile X premutated rCGG repeats, which are responsible for Fragile X-associate tremor/ataxia syndrome (FXTAS), induce nuclear accumulation of mRNAs, including mRNAs involved in stress response, in a *Drosophila* model (Qurashi et al., 2011). Notably, this process is mediated by the interaction of the *Drosophila* homologue of the p68 RNA helicase, Rm62, with Pura, whose localization is profoundly affected by *C9orf72* expression, as shown in this work, and has been suggested to play a pivotal role in *C9orf72*-mediated neurodegeneration in *Drosophila* (Xu et al., 2013). Whether mRNA export defects represent a disease-relevant mechanism in ALS cases caused by *C9orf72*, and how this process might influence the formation of RAN peptides from *C9orf72* translation, an important contributing factor to *C9orf72* toxicity, obviously needs further investigation. However, motor neurons seem to be particularly sensitive to alterations in this process, as mutations in the human *GLE1* gene, that has a central function in nuclear mRNA export, are responsible for the autosomal recessive lethal congenital contracture syndrome-1 (LCCS1), a disease characterized by lack of anterior horn motor neurons and severe atrophy of the ventral spinal cord (Folkmann et al., 2013).

In summary, we have shown here that accumulation of *C9orf72* RNA repeats inside cells is associated with the formation of stress granules, a marked translational repression and a striking accumulation of poly(A) mRNAs in cell nuclei. Our data therefore extend to *C9orf72*-dependent ALS the emerging concept that stress-granule-associated translational repression has a prominent role in neurodegenerative disorders, including ALS, and raise the intriguing possibility that the hexanucleotide expansion in *C9orf72* might interfere with the cellular trafficking of poly(A) RNAs, thus increasing our current understanding of the molecular mechanisms underlying the pathogenesis of familial ALS.

MATERIALS AND METHODS
DNA synthesis and plasmid construction
CC(GGGGCC)$_2$GGGG and CCGG(CCCCGG)$_2$CC DNA fragments were synthesized with a 5′ phosphate (Sigma). Complementary DNA strands were incubated at 95℃ for 5 min in the presence of 100 mM potassium acetate, 2 mM magnesium acetate and 30 mM Hepes-KOH pH 7.4, then slowly cooled to 65℃. After 30 min, the reaction was further cooled to 4℃. 3 µg of annealed oligonucleotides were ligated at room temperature for 24 h by T4 DNA ligase (Promega) and then separated on 1% agarose gel. DNA fragments with different lengths were extracted and cloned into the *Xma*I site of pPCR-Script AmpSK(+) vector (Agilent Technologies). Plasmids containing ten and 31 repeats were obtained and verified by automated sequencing. The hexanucleotide repeats were subcloned into the *Eco*RV/*Not*I sites of pcDNA5/FRT/TO expression vector (Invitrogen) and into the *Bgl*II/*Hin*dIII sites of pEGFP vector (Clontech). For subcellular distribution of poly(A) mRNAs, the repeats were inserted into *Not*I/*Bgl*II sites of pSUPER.retro.puro (Oligoengine), which contains an RNA polymerase III promoter and was previously modified for the

presence of a transcription termination (six thymidine residues immediately downstream the cloning site).

For (TTC)$_{270}$ cloning, a 1300-bp DNA fragment containing 270 Friedreich's-ataxia-associated repeats of a GAA sequence was PCR-amplified from genomic DNA from a human carrier and cloned into pGEM-T Easy Vector (Promega). *Not*I fragments were then inserted into pcDNA5/FRT/TO vector. Sequence orientation was controlled by restriction analysis of each vector and verified by automated sequencing, and the reverse orientation containing a 5′-(TTC)$_{270}$-3′ repeat was used for the experiments.

Cell culture and transfection
Mouse motor neuron-like NSC34 cells were grown in Dulbecco's modified Eagle's medium (DMEM) with F12 (Invitrogen) supplemented with 10% fetal bovine serum (tetracycline free, Lonza) at 37℃ in an atmosphere of 5% CO_2 in air. Human neuroblastoma SH-SY5Y cells and cervical carcinoma HeLa cells were grown in DMEM (Invitrogen) supplemented with 10% fetal bovine serum (Invitrogen) at 37℃ in an atmosphere of 5% CO_2 in air. For transient expression of hexanucleotide repeats, NSC34 and HeLa cells were transfected with pcDNA5-(G4C2)$_{10}$, pcDNA5-(G4C2)$_{31}$ and pcDNA5-(TTC)$_{270}$ using Lipofectamine Plus reagent (Invitrogen) according to the manufacturer's instruction.

qRT-PCR analysis
For quantitative real-time PCR (qRT-PCR), RNAs were isolated using TRIzol (Invitrogen) and treated with DNase. RNAs were quantified and reverse-transcribed with random primers according to an ImProm II reverse transcriptase kit (Promega). qRT-PCR was performed with LightCycler 480 SYBR Green I Master Mix (Roche). A 113-bp sequence of pcDNA5/FRT/TO upstream of the repeat cloning sites was amplified using the following primers: forward, 5′-CGCAAATGGGCGGTA-GGCGTG-3′; reverse, 5′-CACTAAACGAGCTCGTCGACG-3′. Actin was also measured as a housekeeping gene.

RNA transcription *in vitro* and pulldown assay
pPCR-Script-(G4C2)$_{31}$ and pGEM-(TTC)$_{270}$ vectors were linearized with *Sac*I or *Sal*I, respectively, and used as a template for *in vitro* RNA transcription, that was performed with RNAMaxx High Yield Transcription Kit (Agilent Technologies) in the absence or presence of biotin-14-CTP (Invitrogen) in a one-to-one ratio of normal to modified cytosine, following the manufacturer's instructions. After treatment with RNase-free DNase (Promega), RNA transcripts were purified with phenol:chloroform:isoamyl alcohol (25:24:1; Invitrogen). RNA was denatured at 90℃ for 2 min, and incubated for 1 h at room temperature in the presence of 100 mM KCl, 10 mM $MgCl_2$ and 10 mM Tris-HCl pH 7.4.

For the pulldown assay, mouse brain and spinal cords were homogenized using a Teflon homogenizer for 30 s on ice in lysis buffer (250 mM NaCl, 20 mM Tris-HCl, pH 7.4, 0.5% Nonidet-P40, 0.5 mM DTT, 1 mM PMSF, protease inhibitor cocktail from Sigma-Aldrich). NSC34 and SH-SY5Y cell lysis was performed in the same buffer. All animal experiments were performed according to approved guidelines.

A clear supernatant was obtained by centrifugation of cell and tissue lysates twice at 20,000 *g* for 5 min. Protein content was determined using a Bradford protein assay (Bio-Rad). 1 mg of total protein extract was diluted in 0.5 ml of lysis buffer with a final NaCl concentration of 150 mM, and then pre-cleared with 60 µl of Dynabeads® M-280 Streptavidin (Invitrogen) for 30 min. The pre-cleared protein extract was incubated for 1 h with 5 µg of biotinylated (G4C2)$_{31}$ RNA, and then with 60 µl of Dynabeads® M-280 Streptavidin for 1 h. After five washes in lysis buffer, RNA–protein complexes were resuspended in 2× Laemmli sample buffer, boiled for 5 min and subjected to 4–12% NuPAGE gel elecrophoresis (Invitrogen). A non-biotinylated (G4C2)$_{31}$ RNA was also pulled-down and analyzed in the same conditions to check for unspecific binding of proteins. Gels were stained with Coomassie Blue for the following mass spectrometry analysis or subjected to western blot analysis.

Protein identification by mass spectrometry analysis

Bands from gels were processed by tryptic proteolysis, after reduction and alkylation steps. The peptide mixtures were analyzed by matrix-assisted laser-desorption ionization–time-of-flight (MALDI-ToF) mass spectrometry (AutoFlexII, BrukerDaltonics) and the resulting peptide mass fingerprints were used to identify proteins with the Mascot search engine (Palermo et al., 2012).

All peptide mixtures were also analyzed by a nano LCLTQ-Orbitrap mass spectrometer platform. After desalting (Rappsilber et al., 2007) and resuspension in 0.1% of formic acid, samples were loaded from an autosampler onto a 10-cm long silica capillary packed with C18 reverse phase resin, using the Dionex Ultimate 3000 system (LC Packings, Dionex, Amsterdam, The Netherlands). The elution of peptides was monitored by a linear ion trap-orbitrap hybrid mass spectrometer (LTQ-Orbitrap Discovery, Thermo Fisher Scientific) equipped with a nanoelectrospray ion source (Thermo Fisher Scientific), operating in the positive ionization mode with a spray voltage of 1.9 kV. In data-dependent tandem mass spectrometry (MS/MS) scans, the five most abundant ions were fragmented by collision-induced dissociation (CID) and analyzed in the linear trap. Data acquisition was controlled by Xcalibur 2.1. The MS/MS spectra were searched by MaxQuant (v. 1.4.1) against the mouse UniProtKB FASTA database. The identifications with only one unique peptide were accepted.

Fluorescence in situ hybridization and immunofluorescence analysis

Cell cultures were grown on poly-L-lysine-coated glass coverslips, washed in PBS and fixed with 4% paraformaldehyde in PBS for 10 min. Cells were then washed twice with 70% ethanol and stored in 70% ethanol at 4℃. Cells were rehydrated with 5 mM $MgCl_2$ in PBS for 30 min and then pre-hybridized in 35% formamide, 10 mM sodium phosphate pH 7.0, and 2×SSC (300 mM NaCl, 30 mM sodium citrate) for 30 min at room temperature. For the probe hybridization, cells were incubated with 250 ng/ml of Cy3-labeled $(C4G2)_4$ (Sigma) and/or Cy5-conjugated oligo(dT) in 30% formamide, 10% dextrane sulphate, 2× SSC, 0.2% BSA, 10 mM sodium phosphate pH 7.0, and 0.5 mg/ml each of E. coli tRNA and sonicated salmon sperm DNA, at 37℃ overnight in a humidified chamber. After hybridization, cells were washed twice with 35% formamide, 10 mM sodium phosphate, pH 7.0, and 2× SSC for 30 min each at 37℃; twice with 2× SSC, 0.1% Triton-X100, 15 min each at room temperature; and twice with 0.2×SSC, 0.1% Triton X-100, 15 min each at room temperature. After washing, coverslips were mounted on the slides, or processed for immunofluorescence analysis as follows.

Cells were blocked for 30 min in PBS, 1% BSA and incubated for 1 h at 37℃ with primary antibodies (see below) diluted in the same buffer. Cells were washed in PBS and incubated for 45 min with fluorophore-conjugated secondary antibodies diluted in PBS, 1% BSA. After rinsing in PBS, cells were stained with 1 µg/ml DAPI (Sigma) and examined with a Zeiss LSM 510 Confocal Laser Scanning Microscope equipped with a 63× objective. Fluorescence images were processed using ZEN 2009 (Carl Zeiss) and Adobe Photoshop software.

Protein extraction

After rinsing with ice-cold PBS, cells were lysed in RIPA buffer (50 mM Tris-HCl, pH 7.4, 1% Triton X-100, 0.25% Na-deoxycholate, 0.1% SDS, 150 mM NaCl, 1 mM EDTA and 5 mM $MgCl_2$) containing a protease inhibitor cocktail (Sigma). A clear supernatant was obtained by centrifugation of lysates at 17,000 g for 10 min. Protein content was determined using Bradford protein assay (Bio-Rad).

For eIF2α phosphorylation measurement, cells were treated with 1 mM sodium orthovanadate for 30 min, then cell lysis was performed in RIPA buffer containing a protease inhibitor cocktail (Sigma), 1 mM sodium orthovanadate and 50 mM sodium fluoride.

For translation rate measurement, prior of cell lysis, cell cultures were treated with 10 µg/ml puromycin for 10 min. Where specified, cells were previously treated with 1 mM cycloheximide for 10 min.

Nuclear–cytosolic fractionation

After 24 h from transfection, HeLa cells were harvested, washed in ice-cold PBS and lysed in low-salt buffer (10 mM Hepes, pH 7.4, 42 mM KCl, 5 mM $MgCl_2$, 0.5% CHAPS, 1 mM DTT, 1 mM PMSF and 1 µg/ml leupeptin). After 10 min on ice, lysates were centrifuged at 2000 g for 10 min. Supernatants were collected as cytosolic fractions, whereas pellets were resuspended in high-salt buffer (50 mM Tris-HCl pH 7.4, 400 mM NaCl, 1 mM EDTA, 1% Triton X-100, 0.5% Nonidet-P40, 10% glycerol, 2 mM DTT, 1 mM PMSF, protease inhibitor cocktail from Sigma-Aldrich). After 30 min on ice, lysates were centrifuged at 20,000 g for 15 min and supernatants were collected as nuclear fractions.

Electrophoresis and western blotting

Protein samples were separated by SDS-PAGE and transferred onto nitrocellulose membranes (Amersham). Membranes were blocked for 1 h in Tris-buffered saline solution with 0.1% Tween-20 (TBS-T) containing 5% non-fat dry milk, and then incubated for 2 h at room temperature or overnight at 4℃ with indicated primary antibodies, diluted in TBS-T containing 2% non-fat dry milk. After rinsing with TBS-T solution, membranes were incubated for 1 h with the appropriated peroxidase-conjugated secondary antibody diluted in TBS-T containing 1% non-fat dry milk, then washed and developed using the ECL chemiluminescence detection system (Roche). Densitometric analyses were performed using ImageJ software program (National Institutes of Health).

Antibodies and reagents

The following antibodies were used: anti-hnRNP H, anti-RAX and anti-laminB goat polyclonal antibodies (Santa Cruz Biotechnology); anti-hnRNP U (H-94) rabbit polyclonal antibody (Santa Cruz Biotechnology); anti-ILF2 (G-3), anti-SRSF1 (96), anti-PABP (10E10) mouse monoclonal antibodies (Santa Cruz Biotechnology); anti-eIF2α (D7D3), anti-phospho-eIF2α (D9G8) rabbit monoclonal antibodies (Cell Signaling); anti-eIF2β rabbit polyclonal antibody (GeneTex); anti-ILF3 (EPR3626) rabbit monoclonal antibody (GeneTex); anti-FUS rabbit polyclonal antibody (Bethyl Laboratories); anti-TDP43 rabbit polyclonal antibody (ProteinTech); anti-β-actin mouse monoclonal antibody (Sigma); anti-Puromycin (12D10) mouse monoclonal antibody (Millipore); anti-MBNL1 mouse monoclonal (P11) antibody (a kind gift of Annalisa Botta, Dipartimento di Biomedicina e Prevenzione, University of Rome Tor Vergata, Italy); anti-hnRNP A2/B1 mouse monoclonal antibody (GeneTex); anti-FMRP rabbit polyclonal (Ram2) antibody; anti-TIAR mouse monoclonal antibody (BD Transduction Lab); anti-Pura mouse monoclonal antibody (Abcam, ab77734); anti-Pura rabbit polyclonal antibody (Abcam, ab79936). Anti-rabbit, anti-mouse and anti-goat IgG peroxidase-conjugated secondary antibodies were from Bio Rad; Alexa-Fluor-conjugated secondary antibodies were from Invitrogen. Anti-mouse IgG conjugated to Cy3 was from Jackson ImmunoResearch Laboratories. Poly-U, Poly-G, sodium arsenite, thapsigargin, puromycin and cyclohexymide were from Sigma. PERK inhibitor GSK2606414 was from Calbiochem. tRNA was from Roche, and single-stranded (ss)DNA from Sigma.

Statistical analysis

Statistical analysis was performed with an unpaired two-tailed Student's t-test. Values significantly different from the relative control are indicated with asterisks. P-values of 0.05 or 0.01 were considered significant.

Competing interests
The authors declare no competing or financial interests.

Supplementary material

Supplementary material available online at
http://jcs.biologists.org/lookup/suppl/doi:10.1242/jcs.165332/-/DC1

References

Achsel, T., Barabino, S., Cozzolino, M. and Carrì, M. T. (2013). The intriguing case of motor neuron disease: ALS and SMA come closer. *Biochem. Soc. Trans.* **41**, 1593-1597.

Bagni, C. and Oostra, B. A. (2013). Fragile X syndrome: from protein function to therapy. *Am. J. Med. Genet. A.* **161**, 2809-2821.

Bentmann, E., Haass, C. and Dormann, D. (2013). Stress granules in neurodegeneration – lessons learnt from TAR DNA binding protein of 43 kDa and fused in sarcoma. *FEBS J.* **280**, 4348-4370.

Burgess, H. M., Richardson, W. A., Anderson, R. C., Salaun, C., Graham, S. V. and Gray, N. K. (2011). Nuclear relocalisation of cytoplasmic poly(A)-binding proteins PABP1 and PABP4 in response to UV irradiation reveals mRNA-dependent export of metazoan PABPs. *J. Cell Sci.* **124**, 3344-3355.

Chen, M. and Manley, J. L. (2009). Mechanisms of alternative splicing regulation: insights from molecular and genomics approaches. *Nat. Rev. Mol. Cell Biol.* **10**, 741-754.

Cooper-Knock, J., Walsh, M. J., Higginbottom, A., Robin Highley, J., Dickman, M. J., Edbauer, D., Ince, P. G., Wharton, S. B., Wilson, S. A., Kirby, J. et al. (2014). Sequestration of multiple RNA recognition motif-containing proteins by C9orf72 repeat expansions. *Brain* **137**, 2040-2051.

DeJesus-Hernandez, M., Mackenzie, I. R., Boeve, B. F., Boxer, A. L., Baker, M., Rutherford, N. J., Nicholson, A. M., Finch, N. A., Flynn, H., Adamson, J. et al. (2011). Expanded GGGGCC hexanucleotide repeat in noncoding region of C9ORF72 causes chromosome 9p-linked FTD and ALS. *Neuron* **72**, 245-256.

Donnelly, C. J., Zhang, P. W., Pham, J. T., Haeusler, A. R., Mistry, N. A., Vidensky, S., Daley, E. L., Poth, E. M., Hoover, B., Fines, D. M. et al. (2013). RNA toxicity from the ALS/FTD C9ORF72 expansion is mitigated by antisense intervention. *Neuron* **80**, 415-428.

Folkmann, A. W., Collier, S. E., Zhan, X., Aditi, O. h., i, M. D. and Wente, S. R. (2013). Gle1 functions during mRNA export in an oligomeric complex that is altered in human disease. *Cell* **155**, 582-593.

Gendron, T. F., Belzil, V. V., Zhang, Y. J. and Petrucelli, L. (2014). Mechanisms of toxicity in C9FTLD/ALS. *Acta Neuropathol.* **127**, 359-376.

Haeusler, A. R., Donnelly, C. J., Periz, G., Simko, E. A., Shaw, P. G., Kim, M. S., Maragakis, N. J., Troncoso, J. C., Pandey, A., Sattler, R. et al. (2014). C9orf72 nucleotide repeat structures initiate molecular cascades of disease. *Nature* **507**, 195-200.

Kedersha, N., Cho, M. R., Li, W., Yacono, P. W., Chen, S., Gilks, N., Golan, D. E. and Anderson, P. (2000). Dynamic shuttling of TIA-1 accompanies the recruitment of mRNA to mammalian stress granules. *J. Cell Biol.* **151**, 1257-1268.

Kim, H. J., Raphael, A. R., LaDow, E. S., McGurk, L., Weber, R. A., Trojanowski, J. Q., Lee, V. M., Finkbeiner, S., Gitler, A. D. and Bonini, N. M. (2014). Therapeutic modulation of eIF2α phosphorylation rescues TDP-43 toxicity in amyotrophic lateral sclerosis disease models. *Nat. Genet.* **46**, 152-160.

Kumar, G. R. and Glaunsinger, B. A. (2010). Nuclear import of cytoplasmic poly(A) binding protein restricts gene expression via hyperadenylation and nuclear retention of mRNA. *Mol. Cell. Biol.* **30**, 4996-5008.

La Spada, A. R. and Taylor, J. P. (2010). Repeat expansion disease: progress and puzzles in disease pathogenesis. *Nat. Rev. Genet.* **11**, 247-258.

Lee, Y. B., Chen, H. J., Peres, J. N., Gomez-Deza, J., Attig, J., Stalekar, M., Troakes, C., Nishimura, A. L., Scotter, E. L., Vance, C. et al. (2013). Hexanucleotide repeats in ALS/FTD form length-dependent RNA foci, sequester RNA binding proteins, and are neurotoxic. *Cell Reports* **5**, 1178-1186.

McGurk, L., Lee, V. M., Trojanowksi, J. Q., Van Deerlin, V. M., Lee, E. B. and Bonini, N. M. (2014). Poly-A binding protein-1 localization to a subset of TDP-43 inclusions in amyotrophic lateral sclerosis occurs more frequently in patients harboring an expansion in C9orf72. *J. Neuropathol. Exp. Neurol.* **73**, 837-845.

Mizielinska, S., Lashley, T., Norona, F. E., Clayton, E. L., Ridler, C. E., Fratta, P. and Isaacs, A. M. (2013). C9orf72 frontotemporal lobar degeneration is characterised by frequent neuronal sense and antisense RNA foci. *Acta Neuropathol.* **126**, 845-857.

Mokas, S., Mills, J. R., Garreau, C., Fournier, M. J., Robert, F., Arya, P., Kaufman, R. J., Pelletier, J. and Mazroui, R. (2009). Uncoupling stress granule assembly and translation initiation inhibition. *Mol. Biol. Cell* **20**, 2673-2683.

Mori, K., Lammich, S., Mackenzie, I. R., Forné, I., Zilow, S., Kretzschmar, H., Edbauer, D., Janssens, J., Kleinberger, G., Cruts, M. et al. (2013). hnRNP A3 binds to GGGGCC repeats and is a constituent of p62-positive/TDP43-negative inclusions in the hippocampus of patients with C9orf72 mutations. *Acta Neuropathol.* **125**, 413-423.

Palermo, R., Checquolo, S., Giovenco, A., Grazioli, P., Kumar, V., Campese, A. F., Giorgi, A., Napolitano, M., Canettieri, G., Ferrara, G. et al. (2012). Acetylation controls Notch3 stability and function in T-cell leukemia. *Oncogene* **31**, 3807-3817.

Qurashi, A., Li, W., Zhou, J. Y., Peng, J. and Jin, P. (2011). Nuclear accumulation of stress response mRNAs contributes to the neurodegeneration caused by Fragile X premutation rCGG repeats. *PLoS Genet.* **7**, e1002102.

Rappsilber, J., Mann, M. and Ishihama, Y. (2007). Protocol for micro-purification, enrichment, pre-fractionation and storage of peptides for proteomics using StageTips. *Nat. Protoc.* **2**, 1896-1906.

Reddy, K., Zamiri, B., Stanley, S. Y., Macgregor, R. B., Jr and Pearson, C. E. (2013). The disease-associated r(GGGGCC)n repeat from the C9orf72 gene forms tract length-dependent uni- and multimolecular RNA G-quadruplex structures. *J. Biol. Chem.* **288**, 9860-9866.

Renton, A. E., Majounie, E., Waite, A., Simón-Sánchez, J., Rollinson, S., Gibbs, J. R., Schymick, J. C., Laaksovirta, H., van Swieten, J. C., Myllykangas, L. et al.; ITALSGEN Consortium (2011). A hexanucleotide repeat expansion in C9ORF72 is the cause of chromosome 9p21-linked ALS-FTD. *Neuron* **72**, 257-268.

Schmidt, E. K., Clavarino, G., Ceppi, M. and Pierre, P. (2009). SUnSET, a nonradioactive method to monitor protein synthesis. *Nat. Methods* **6**, 275-277.

Smith, R. W. and Gray, N. K. (2010). Poly(A)-binding protein (PABP): a common viral target. *Biochem. J.* **426**, 1-12.

Smith, R. W., Blee, T. K. and Gray, N. K. (2014). Poly(A)-binding proteins are required for diverse biological processes in metazoans. *Biochem. Soc. Trans.* **42**, 1229-1237.

Spriggs, K. A., Bushell, M. and Willis, A. E. (2010). Translational regulation of gene expression during conditions of cell stress. *Mol. Cell* **40**, 228-237.

Stepto, A., Gallo, J. M., Shaw, C. E. and Hirth, F. (2014). Modelling C9ORF72 hexanucleotide repeat expansion in amyotrophic lateral sclerosis and frontotemporal dementia. *Acta Neuropathol.* **127**, 377-389.

Walsh, M. J., Cooper-Knock, J., Dodd, J. E., Stopford, M. J., Mihaylov, S. R., Kirby, J., Shaw, P. J. and Hautbergue, G. M. (2015). Invited review: Decoding the pathophysiological mechanisms that underlie RNA dysregulation in neurodegenerative disorders: a review of the current state of the art. *Neuropathol. Appl. Neurobiol.* **41**, 109-134.

White, M. K., Johnson, E. M. and Khalili, K. (2009). Multiple roles for Puralpha in cellular and viral regulation. *Cell Cycle* **8**, 414-420.

Xu, Z., Poidevin, M., Li, X., Li, Y., Shu, L., Nelson, D. L., Li, H., Hales, C. M., Gearing, M., Wingo, T. S. et al. (2013). Expanded GGGGCC repeat RNA associated with amyotrophic lateral sclerosis and frontotemporal dementia causes neurodegeneration. *Proc. Natl. Acad. Sci. USA* **110**, 7778-7783.